

Cross-pore electrostatic repulsions are critical for stabilizing the GABA_A receptor open state

Sruthi Murlidaran,* Reza Salari,* †
Grace Brannigan * †

*Center for Computational and Integrative Biology, Rutgers University-Camden,
Camden, NJ 08102, †Department of Physics, Rutgers University-Camden,
Camden, NJ 08102

Abstract

INTRODUCTION

Pentameric Ligand-gated Ion Channels (pLGICs) are essential components of the post-synaptic membrane, serving both inhibitory and excitatory roles. pLGIC sequence varies significantly within and between prokaryotes and eukaryotes,(1) with typical homologies of about 30%. pLGIC function can be quite sensitive to even small differences in sequence, but numerous pLGIC structures have now demonstrated significant structural conservation despite functional variation. This property has made it challenging to isolate the roles of various pLGIC components or sequence variations in subtle functional effects.

Despite the high sequence variation among pLGIC subunits, even for those forming a heteromeric channel, few single nucleotide polymorphisms (SNPs) are found among populations within coding regions for a specific subunit. Mutations causing loss of function in inhibitory receptors or gain of function in excitatory receptors can result in seizures induced by neuron overexcitation. Many naturally occurring mutations are associated with various forms of epilepsy(2–5), with several relevant mutations identified even before the use of genome-wide association studies. The molecular mechanisms underlying the effect of nearly all mutations on signaling are unknown.

GABA is the primary inhibitory neurotransmitter in the central nervous system; inhibition is partially transduced by extracellular binding to the type A GABA receptor, an anionic pLGIC(6–8). Many molecules with sedative, anxiolytic, and anesthetic properties are positive modulators of the GABA_AR, including neurosteroids(9–13), benzodiazepines(14), and inhalational and intravenous general anesthetics(15–17). Negative modulators, such as pregnenolone sulfate(18), can induce seizures, as can certain mutations. Seizures associated with inherited mutations typically require conditions that are found only infrequently; survival is unlikely in the presence of consistent seizures. GABA_AR receptors with these mutations are therefore known *a priori* to be functional

under typical conditions but dysfunctional under well-defined alternate conditions, making them promising candidates for identifying the role of the mutated residue.

Each subunit consists of an extracellular agonist-binding domain (ECD) and a transmembrane domain containing a four helix bundle with helices labeled (M1-M4). The M2 helices line the pore, and the M2-M3 loop connecting the M2 and M3 helices interacts directly with the ECD. The loop has long been hypothesized to "communicate" agonist binding to the transmembrane domain,(19–27) with several mutation studies indicating the importance for agonist sensitivity of short-range attractive electrostatic interactions, such as salt-bridges, between the M2-M3 loop and the ECD. (28–31)

In GABA_AR subunits the M2-M3 loop contains a basic residue appearing at the homologous positions of α 279, β 274, or γ 289, notated as M2 24' in the prime numbering scheme suggested in (1). Harrison and colleagues(30) demonstrated that charge-reversal of α 279 reduced agonist sensitivity (EC50) which was restorable via additional charge-reversal of α D57 or α D149, both within the ECD and expected to be near the M2-M3 loop. Maximum whole-cell current, however, was reduced by about 1/3 upon the single α D279K mutation, and further reduced by about the same amount with the second mutation of α D57K or α D149K, suggesting a significant role for α 279K in stabilizing the open state beyond forming a salt-bridge with the ECD. Similar behavior was observed in the nicotinic acetylcholine receptor (nAChR), upon charge-reversal of α R209 in M1 and α E45 in the ECD.(25)

A natural but uncommonly occurring SNP at the homologous residue in the γ subunit (γ 2 K289), further suggests an additional role for this residue beyond gating, because the γ subunit does not form GABA binding cavities. The γ 2:K289M mutation has been reported in families with generalized epilepsy and febrile seizures plus(GEFS+)(2, 32, 33), a generalized phenotype that often includes only febrile (fever-caused) seizures until about age 11, but can also include less severe myoclonic, atonic, or absence seizures at normal body temperature. In $\alpha_1\beta_2\gamma_2$ K289M receptors, GABA-evoked current amplitude was dramatically reduced relative to the WT (33, 34), while in $\alpha_1\beta_3\gamma_2$ K289M receptors the mutation did not affect current amplitudes but did increase the deactivation rate(35). In the latter receptors, currents had reduced mean open times, in part due to flickering(2, 31, 36). In hippocampal neurons containing GABA_AR with γ 2:K289M subunits accelerated deactivation of inhibitory post synaptic currents was also observed(35).

Little information has been available regarding the effect of the mutation on GABA_AR structure and dynamics. Using a homology model of the GABA_AR receptor based on the medium resolution cryo electron microscopy structure of the nicotinic Acetylcholine Receptor (nAChR), Brownian Dynamics Simulations of ion conduction were used to suggest that mutant receptors display reduced conductance due to reduced affinity of the ion for the ion channel(37). However, the recent x-ray structures of eukaryotic and prokaryotic homologs have suggested that alignment of the sequence with the electron density map in the M2 helices is likely incorrect in the structure used for these simulations. Furthermore, these simulations do not contain explicit representations of water or lipid molecules.

The temperature dependence of this mutation suggests a significant role for entropy and conformational fluctuations in determining its effects. Here we conduct molecular dynamics simulations with multiple replicas of the γ 2 K289 and M289 forms of the receptor, at both lower and higher temperatures. We observe a moderately narrowed pore in the M289 receptor at 300K, and a significantly narrowed pore at 315K. Through adaptive biasing force (ABF) calculations, we demonstrate that the effects at 315K result in a substantially higher barrier for conduction of a chloride ion.

$\gamma 2$ K289 was not observed to form salt bridges with the ECD, and these conformational effects showed no clear correlation to any salt-bridging pattern. We propose instead that the five conserved basic residues at this position form a ring of positive charge that effectively pushes the five M2-M3 loops away from the center, pulling M2 helices with it, and stabilizing the open state. Neutralizing one of the charges as with $\gamma_2 K289M$ reduces this repulsion. When it is combined with a temperature increase that softens the conformational preferences resulting from remaining interactions common to both K and M receptors, the non-temperature dependent change in electrostatic repulsions dominates.

We present a simple variational theory that quantitatively predicts the effect of $\gamma 2:K289M$ on the preferred separation of M2-M3 loop charges, using only the mean and standard deviation of the separation in the wild type $\gamma 2:K289$ channel. Temperature dependence appears through both the effect of temperature on the standard deviation and as a linear term in the theory. The success of the theory supports a critical role for these electrostatic repulsions in stabilizing the wild-type receptor and also in transducing the effects of the mutation.

MATERIALS AND METHODS

Homology Models

A high resolution structure of a GABA_{AR} was not available until the recent publication of 3Å resolution structure for a β_3 homopentamer. In the transmembrane domain, homology between GABA_{AR} α or γ to GABA_{AR} β is not significantly improved relative to homology between GABA_{AR} α/γ subunits and GluCl α (need numbers), and as a result homology models of $\alpha\beta\gamma$ GABA_{AR} built on the GABA_{AR} β_3 homopentamer are not expected to be significantly improved relative to those based on GluCl. The model used in this paper corresponds to Model 1 - CHOL from Reference(38), and was built with GluCl (PDB code : 3RHW) as a template as well as the alignments published in Ref(39). Further justification and details on this model can be found in Reference(38)

System Setup

This manuscript considers data from four simulations at 300K and four simulations at 315K, with 2 wild type (termed K1, K2) and 2 mutant (M1, M2). The systems were prepared as in Ref(38), by embedding the protein in a lipid bilayer composed of 4:1 phosphatidylcholine (POPC) : cholesterol mixture built using CHARMM Membrane builder, with the final system containing 268 POPC and 71 membrane CHOL molecules. In addition to membrane cholesterol, this model includes cholesterol docked to five pseudo-symmetric intersubunit sites, with implications and justification for this decision reported in (38). The systems were solvated using the SOLVATE plugin in VMD(40) and neutralizing ions were added to bring the system to a 0.15M salt concentration using the AUTOIONIZE plugin. The final system contained about 160,000 atoms.

Simulation Methods

All simulations used the CHARMM22-CMAP(41) force field with torsional corrections for proteins. The CHARMM36 model(42, 43) was used for phospholipids, ions, water and cholesterol molecules. Energy minimization and MD simulations were conducted using the NAMD2.9 package(44). All simulations employed periodic boundary conditions, long-ranged electrostatics were handled with

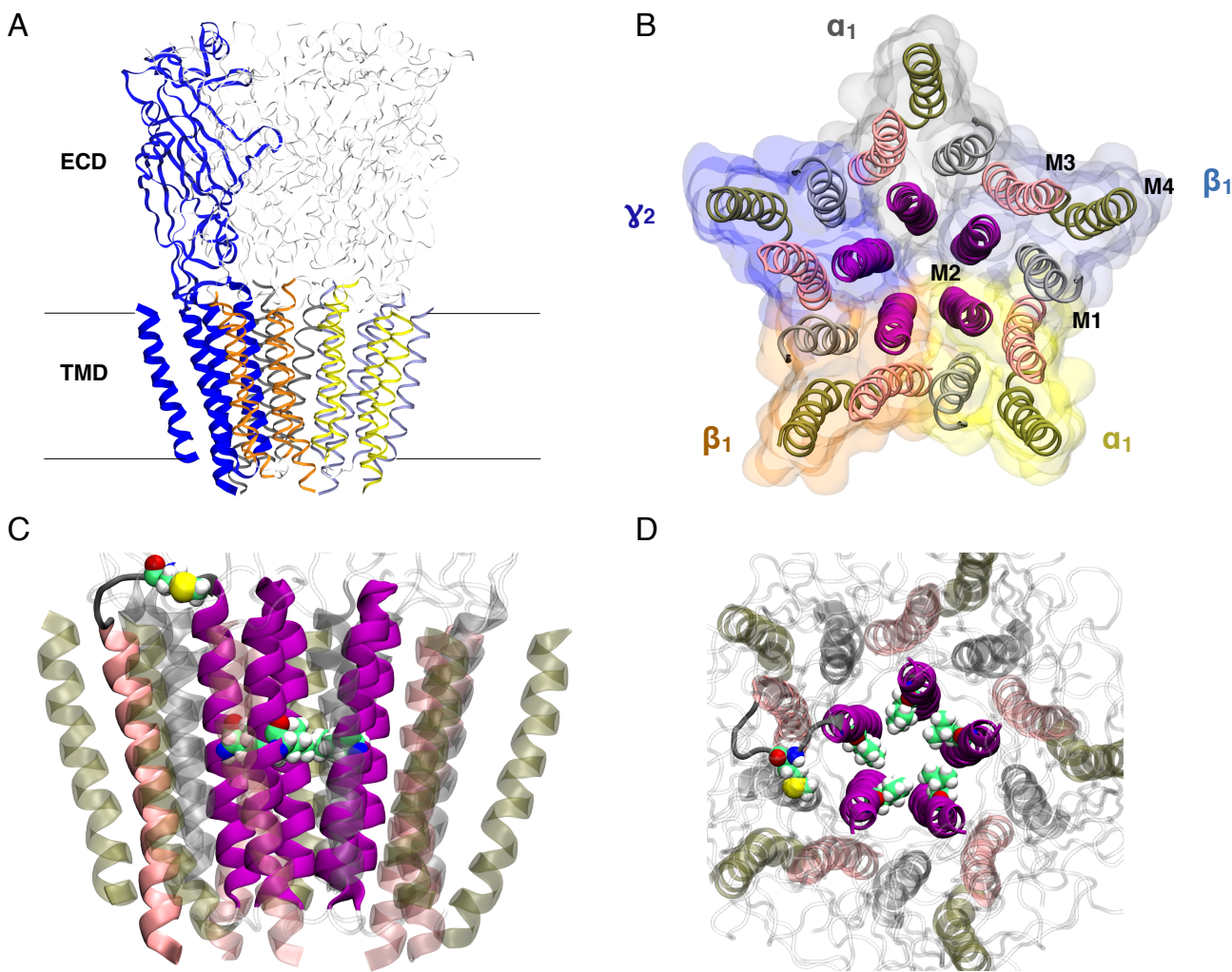


Figure 1: (A) Side View of EC and TM domain showing γ subunit in blue ; (B) View of TM domain, looking down on the membrane from the extracellular region, where each subunit(colored as in A) comprises of a four helix bundle(M1-M4). M1 is gray, M2 is purple, M3 is pink and M4 is ochre; Side view (C) and view from the top-down to (D) the TM domain showing the mutation K289M in the M2-M3 loop and the LEU residues at the 9' location.

smooth particle mesh Ewald method, and a cutoff of 1.2 nm was used for Lennard-Jones potentials with a switching function starting at 1.0 nm. All simulations were run in the NPT ensemble with weak coupling to Langevin thermostat and a barostat at a respective 300 K/315 K and 1 atm. All bonds to the hydrogen atoms were constrained using the SHAKE/RATTLE algorithm. A multiple time-step rRESPA method was used, and controlled with a high frequency time-step of 2fs and low frequency time-step of 4fs. All the systems were energy minimized for 10000 steps, then simulated for 5 ns with restraints of 1 kcal/mol/Å applied to the C_α atoms of the protein. Restraints were then removed and 195 ns of nearly unrestrained simulation was carried out in all four systems. During this period of the simulation, only harmonic restraints (force constant 0.4 kcal/mol/Å) between the intracellular ends of the M3 and M4 helices were used, to mimic the

effects of the intracellular domain and prevent separation of the M4 helix from the rest of the bundle. High temperature (315K) simulations were run for 500 ns following the 200 ns simulations at lower temperature (300K).

Conformational Analysis: Measurement and analysis of the pore radii has been carried out using the HOLE software (45) and TCL scripting through VMD(40). Python scripts have been used to analyze and visualize the hydration of the pore throughout the simulation.

Poisson-Boltzmann Calculations: The Poisson-Boltzmann (PB) profile for conduction of both a Na⁺ and Cl⁻ through the ion channel was calculated using APBSmem(46). The pre-generated PQR format of the proteins using PDB2PQR(47) tool was used as the input for the electrostatic potential calculations. These calculations were performed for initial non-equilibrated structures of the protein, as well as for conformations extracted from the last 50 ns of both the 300K and 315K MD simulations (for Cl⁻).

SMD Simulations: Steered Molecular Dynamics (SMD) simulations (48, 49) were used to obtain favorable positions of the ion at different positions along the channel, for later use in Adaptive Biasing Force (ABF) calculations. The chloride ion was pulled along the pore of the channel at a constant velocity of 10 Å/ns. The force required to pull at constant velocity is also calculated, and can, in principle, be used to calculate a potential of mean force (PMF) using Jarzynski's equation (50, 51), but in practice it is rarely possible to achieve a sufficiently slow pulling speed.

ABF Simulations: Adaptive biasing force calculations (ABF)(52–55) were used to measure the PMF (free energy profile) of a chloride ion translocating the GABA_{AR} ion channel at 315K, for both the WT and K289M channels. ABF was performed using the Collective Variables module(56) of NAMD2.9. The pore axis was divided into 23 bins of each 5 Å length. Initial coordinates for the ion were obtained from SMD simulations. One thousand samples were collected in each bin prior to the application of ABF to avoid undesired non-equilibrium effects on the dynamics. Fifteen ns of trajectory were generated in most bins, while bins near the primary barrier in the pore contained 25 ns.

1 THEORY

The ring of five basic residues can be approximated as five positive charges arranged in a pentamer, each a distance r from the center, which we refer to as the +5 ring. The thermally excited ring may “breathe”, causing r to fluctuate, but for simplicity all charges are treated as equidistant from the center. The variation in r is given by the time-average

$$\delta r^2 = \langle (r(t) - \bar{r})^2 \rangle. \quad (1)$$

At equilibrium, the wild-type receptor exhibits normal fluctuations of r around its time average \bar{r} . The free energy of the wild-type receptor as a function of the +5 ring radius r can be expanded harmonically as

$$H_K(r) = \frac{k_r(r - \bar{r}_K)^2}{2\bar{r}_K}, \quad (2)$$

where the time-average of r is noted by \bar{r}_K , and k_r is the temperature-dependent coefficient governing fluctuations:

$$k_r = \frac{RT \bar{r}_K}{\langle (r - \bar{r}_K)^2 \rangle}, \quad (3)$$

where R is the gas constant and T is the temperature.

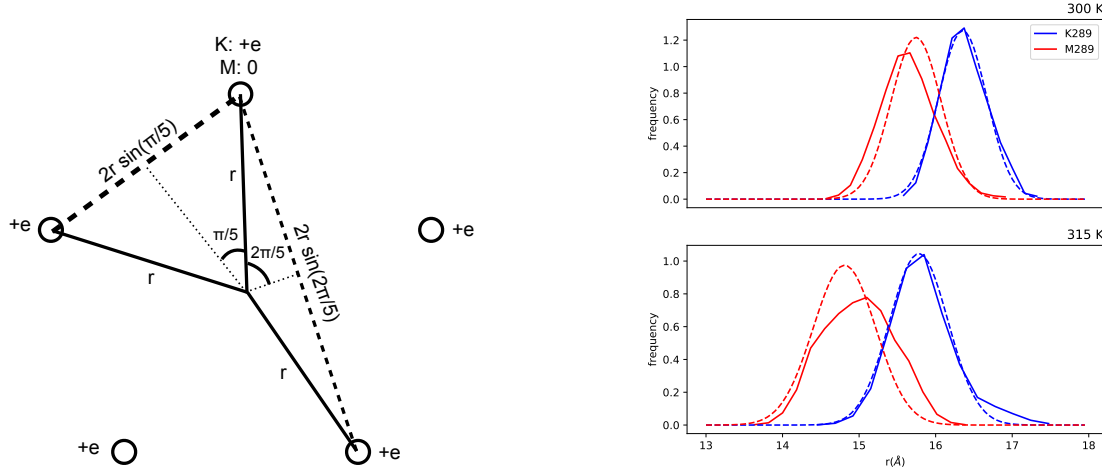


Figure 2: A) A conserved basic residue in the M2-M3 loop yields a pentamer of (un-screened) positive charges, which we refer to as the +5 ring, corresponding to γ K289, α K279, or β K274. The total energy of the +5 ring increases as the ring closes (and r gets smaller), reducing/increasing the distance/repulsion between like-charges. The γ K289M mutation neutralizes one of the charges, yielding a +4 ring, which can shrink with a lowered energetic cost. B) Distributions of r from simulation (solid), a Gaussian fit to K289 (blue dash), and that fit multiplied by the analytically predicted shift $\exp(ck_e e^2 / RTr)$ when one of the charges is removed, and then renormalized (red dash, $c \sim 2.75$).

The mutation γ K289M removes the four long-range repulsive electrostatic interactions involving γ K289. Shrinking the pentameric ring is therefore less unfavorable in the presence of the mutation, and the free energy as a function of r is reduced by the Coulomb energy of the lost interactions:

$$\Delta U(r) = \frac{-k_e e^2}{r} \left(\frac{1}{\sin 2\pi/5} + \frac{1}{\sin \pi/5} \right) = -\frac{ck_e e^2}{r} \quad (4)$$

where $c \sim 2.75$, e is the electron charge, and $k_e = 332 \text{ \AA}/\text{kcal/mol}/e^2$ is the Coulomb constant. Note that this simplification is reasonable primarily because all five charges are nearly coplanar in a plane perpendicular to the pore axis. Other electrostatic interactions will also be lost, but it is reasonable to neglect them because they involve residues screened by another oppositely charged residue, and/or they do not have a significant radial component. The total free energy for the mutant receptor is therefore

$$H_M(r) = H_K(r) + \Delta U(r) \quad (5)$$

$$= \frac{k_r(r - \bar{r}_K)^2}{2\bar{r}_K} - \frac{ck_e e^2}{r} \quad (6)$$

$$= k_r \bar{r}_K \left(\frac{(r - \bar{r}_K)^2}{2\bar{r}_K^2} - \frac{\kappa \bar{r}_K}{r} \right), \quad (7)$$

where

$$\kappa \equiv \frac{c k_e e^2}{k_r \bar{r}_K^2} = \frac{c}{RT} \frac{k_e e^2}{\bar{r}_K} \frac{\delta r^2}{\bar{r}_K^2} \quad (8)$$

The average radius for the mutant receptor, \bar{r}_M , minimizes H_M :

$$\left. \frac{\partial H_M(r)}{\partial r} \right|_{\bar{r}_M} = k_r \left(1 - \frac{\bar{r}_M}{\bar{r}_K} - \kappa \left(\frac{\bar{r}_K}{\bar{r}_M} \right)^2 \right) = 0. \quad (9)$$

Defining the ratio between the two mean radii $\alpha \equiv \bar{r}_M/\bar{r}_K$, Equation 9 reduces to $1 - \alpha - \kappa/\alpha^2 = 0$. This equation has an exact, real solution for $\kappa < 4/27$ ($\frac{k_e e^2}{k_r \bar{r}_K^2} < 0.035$), which when expanded around $\kappa = 0$ is

$$\alpha = \frac{\bar{r}_M}{\bar{r}_K} = 1 - \kappa - 2\kappa^2 - 7\kappa^3 + O(\kappa^4). \quad (10)$$

To first order in κ , we predict that

$$\bar{r}_M = \bar{r}_K - \frac{ck_e e^2}{RT} \frac{\delta r_K^2}{\bar{r}_K^2} \quad (11)$$

where $ck_e e^2/R = 8.3 \times 10^5 \text{ \AA K}$.

RESULTS AND DISCUSSION

Conformational Effects of Mutation

+5 ring

For comparison with the analytical model of the +5 ring presented in Theory, the mean \bar{r}_K and standard deviation $\sqrt{\delta r_K^2}$ of the distance of +5 ring charges from the pore axis (see Figure 2) were measured for the WT systems at each temperature. Results are in Table 1, showing that \bar{r}_K was not sensitive to temperature, while $\sqrt{\delta r_K^2}$ increased with temperature, as expected. These values, as well as Equations 3 and 8, were used to calculate the parameters k_R and κ for each temperature.

Eq. 11 was used to generate predictions for \bar{r}_M , which were reduced relative to \bar{r}_K at both temperatures, but with a much larger reduction at higher temperatures. Quantitative agreement was very good, especially given the simplicity of the theory; at 300K we predicted a 3.1% reduction upon mutation, but obtained a reduction of 2.5%, while at 315K we predicted an 8.2% reduction but obtained a 6.3% reduction. In both cases, the reduction was overestimated, which may reflect computational limits on equilibration time for the K289M receptor, or a higher order contribution to $H_K(r)$ resulting in a steeper free energy cost when $r - \bar{r}_K$ is large.

Pore radius

Although the simple electrostatic effects of neutralizing one charge in the +5 ring predict the observed closing of that ring, a functional effect requires that radius of the +5 ring is coupled to radius of the pore. The pore radius profile (averaged across two replicas) for the K289M and WT receptors is shown in Figure 3. The minimum constriction region (flanked by hydrophobic leucine residues) occurs at roughly the same height along the pore axis for the two systems, but is substantially tighter for the averaged mutant structure, particularly at higher temperatures.

Table 1: Observed values and extracted parameters from analysis of +5 ring in WT receptors, and predicted and observed values upon mutating K289M (yielding +4 ring).

$T(K)$	$\bar{r}_K(\text{\AA})$	$\bar{r}_M(\text{pred, \AA})$	$\bar{r}_M(\text{obs, \AA})$	$\sqrt{\delta r_K^2} (\text{\AA})$	κ	$k_R/\bar{r}_K (\text{kcal/mol}/\text{\AA}^2)$
300	15.9	15.4	15.5	0.27	0.027	8.5
315	15.8	14.5	14.8	0.42	0.066	3.6

As shown in Figure 4, overlap between K289M and WT trajectories (including individual replicas) is substantial at 300K, although the distribution of minimum pore radii is shifted slightly downward (smaller) for the mutant receptor. At 315K, this overlap is substantially reduced, with both WT replicas yielding conformations with persistently larger pore radii than both K289M replicas. These trends mimic those observed in the +5 ring.

Determining whether a single conformation corresponds to an “open” or “closed” state is not typically possible in MD simulations, but we note here that a Cl- atom has a radius of approximately 1.8\AA; at 300K, the minimum pore radius is greater than 1.8\AA for 69% (WT) and 43% (K289M) of the frames, while at 315K, the minimum pore radius is greater than 1.8\AA for 69% (WT) and 26% (K289M) of the frames.

All simulations here were done in the absence of GABA or other agonist, which is not stable in the agonist-binding site due to limitations of classical non-polarizable forcefields for capturing cation-\pi interactions. The presence of agonist would likely alter \bar{r}_K and/or k_R , but would not affect $\Delta U(r)$, which depends only on protein sequence.

Drying of the pore

To further understand the direct implication of the closing of the K289M channel, we measured the average number of water molecules in the pore channel. Many theoretical studies on water have shown that the interfacial drying can be caused by hydrophobic enclosures in the protein(57). Furthermore, studies(58, 59) have also shown that drying of the pore region could lead to blocking of the channel, since water is assumed to facilitate conduction of ions. As mentioned earlier, the pore facing residues in GABA_AR are dominated by non-polar residues and this causes intermittent drying of the channel when the minimum constriction region comes closer to form hydrophobic enclosures. The plot (Figure 5A) shows the density of the water molecules throughout the simulation, along the Z-axis. The figure 5B further substantiates the plot by depicting the absence of water in the minimum constriction region of the pore, at higher temperature, in the K289M systems. Thus, such dehydration of the channel could be a mechanism for inhibiting the conduction of the channel.

Effects of Mutation on Conduction

Electrostatic Barriers in the Channel

The effects of the mutation on purely electrostatic barriers for chloride ion translocation was quantified via the Poisson-Boltzmann equation as described in Methods. The mutation from a

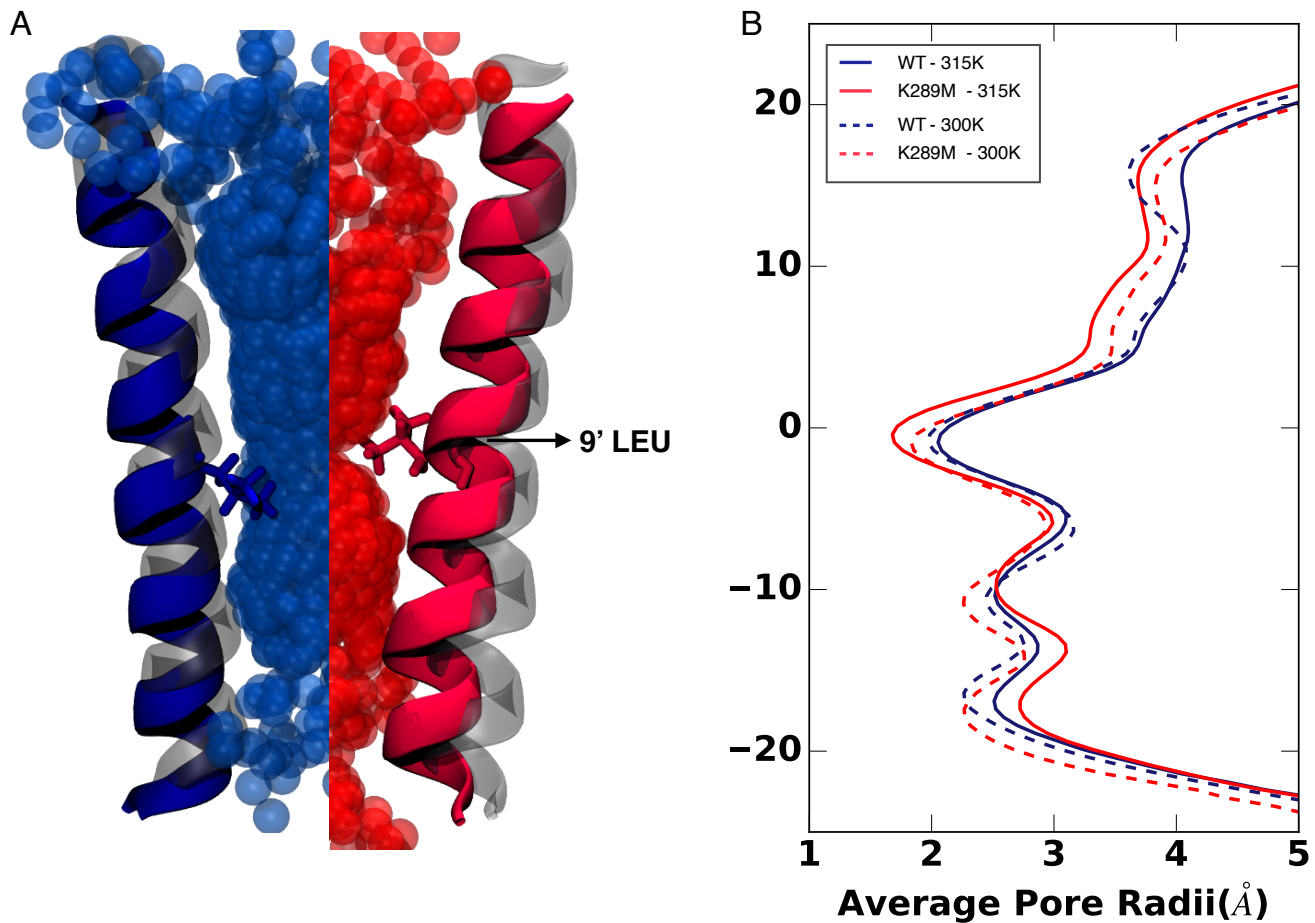


Figure 3: (A) Space-filling models computed from simulations at 315 K, depicting the reduced pore radii of the K289M (red) as compared to that of the WT (blue). (B) Radii of the transmembrane domain along the Z-axis, averaged over all the frames. The pore profile around the 9' region is more constricted at the higher temperature when compared to that of the lower temperature, in both the WT and the K289M. The space filling models further compares the significant reduction in the pore radius in the K289M to the fairly open WT, and the movement of helices compared to their respective initial conformations (gray).

positively charged to neutral residue led to minute changes in the electrostatic profile given identical initial structures (as shown in Supplementary Figure S2(A) and Figure S2(B)), suggesting that the mutation alone could not affect conductance without any conformational changes.

The calculation performed on equilibrated structures of WT and K289M receptors showed a 5–10 kcal/mol (Figure S2(C)) higher electrostatic barrier in K289M, predominantly occurring in the transmembrane domain enclosing the residues containing the minimum pore constriction region. The LEU-gate constriction in addition to the loss of long range electrostatic interactions from K289 seems to contribute to the formation of higher barrier in the K289M. We note that these

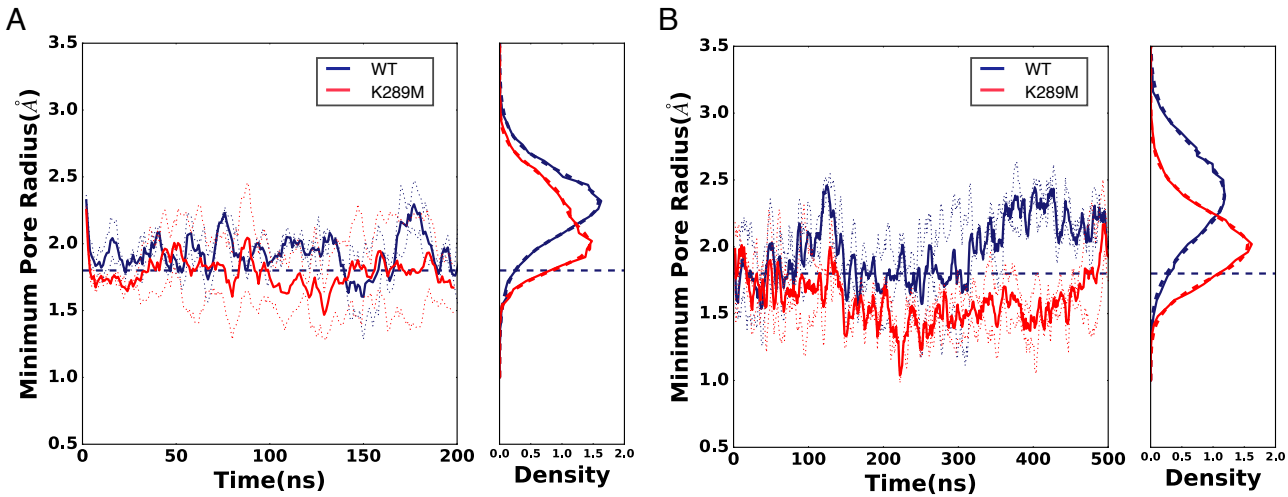


Figure 4: Smoothed time evolution of the pore minimum constriction, averaged (solid lines) over two replicas (dotted lines) each, at 300 K(A) and 315 K(B). The minimum constriction, formed around the 9' region is visibly more constricted for the K289M systems and this reduction is more pronounced at higher temperature. The minimum constriction region in K289M falls below the chloride ion radius of 1.8\AA , thus driving it to a closed state. The probability distribution further shows a clear shift in the peak of the K289M systems towards reduced pore radii at a higher temperature.

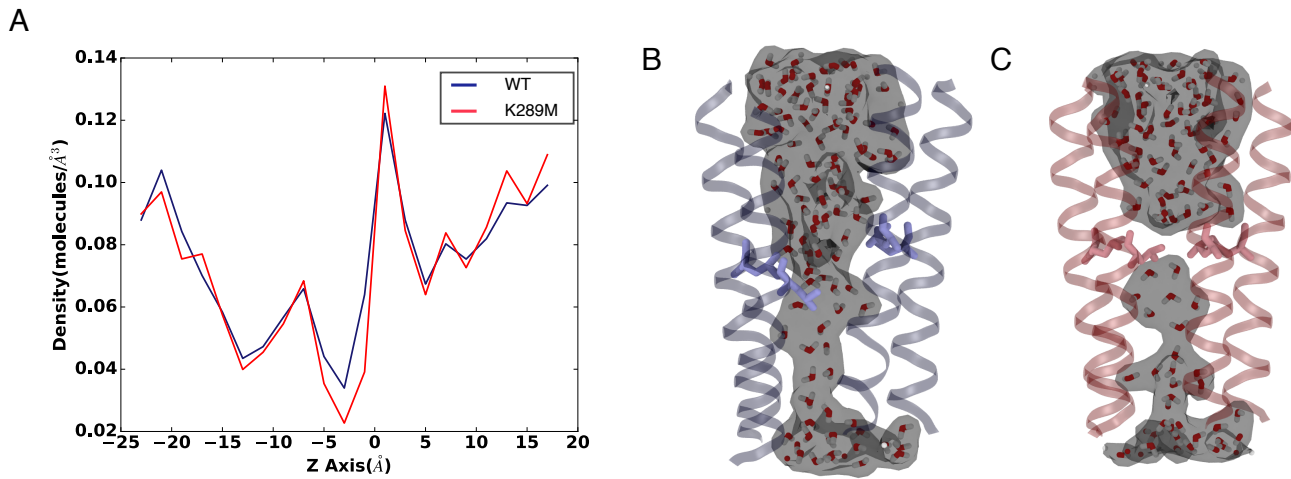


Figure 5: (A)Number of water molecules along the Z-axis averaged over the frames and replicas. Presence of water in the constriction region of the WT - M2 helices (B) as compared to the temporary dryness due to reduction in pore radii in the K289M - M2 helices(C), at higher temperature. On an average, nearly zero no. of water molecules are found at the 9' region in the K289M system, depicting the stripping of water molecules due to the enclosure of the hydrophobic residues.

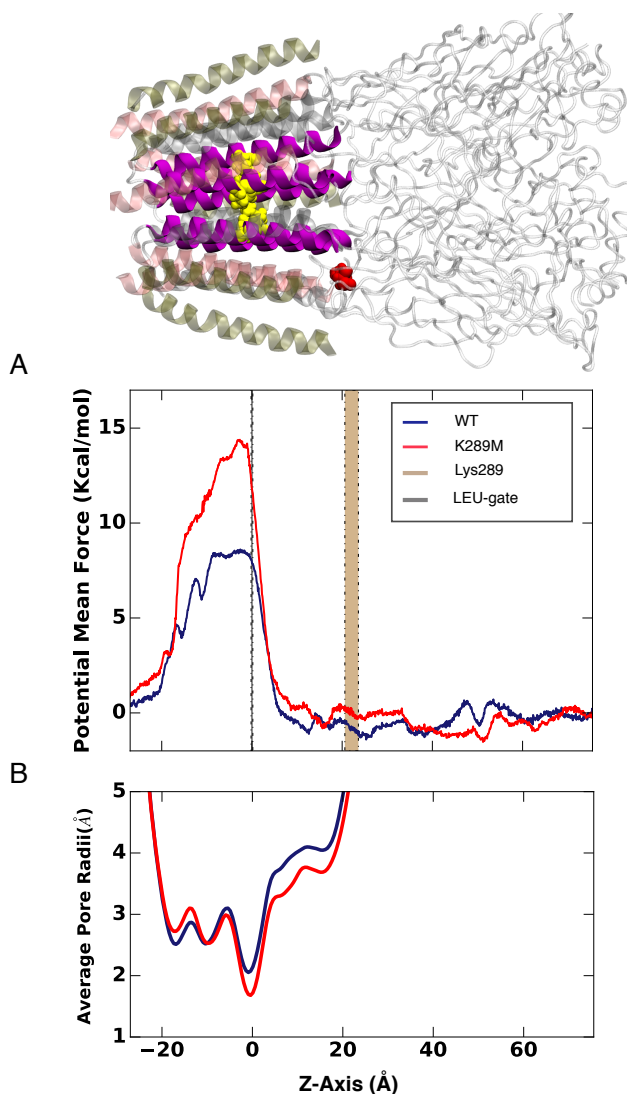


Figure 6: Potential of mean force profile of chloride ion transport (A) Aligned below the horizontally laid protein figure is the plot showing the potential mean force experienced by the ion as it moves through the channel along the Z-axis. (B) These barriers in the channel are further compared with the average pore radius of the TM region of the channel. These comparisons clearly explains that the highest barriers are found at the 9' regions which forms the minimum constriction region. The difference between the barriers at this region is approximately 5 Kcal/mol.

calculations includes electrostatic contributions, but not van der Waals or entropic contributions; these terms are included in the measurement of the potential of mean force via Adaptive Biasing Force calculations as described subsequently.

Potential of Mean Force

The PMF for chloride ion translocation at 315K, measured using ABF, is shown in Figure 6. The largest barrier occurs more proximal to the leucine residues forming the tightest constriction; this

barrier is increased by 5 kcal/mol for the mutant receptors. A slight, broad well (relative to a reference position outside the receptor) is apparent around residue 289 in the PMF for the WT receptor, while at the same location in the K289M receptor the PMF is slightly elevated relative to the reference location. However, these differences are slight compared to the effects of the mutation on the primary barrier, indicating that while mutation of a positively charged to neutral residue does have a small effect on affinity of the chloride ion for the region of the receptor near the mutation, the dominant effect of the mutation on conduction is via conformational instability of the open state.

CONCLUSION

In this work, we investigated the effects of a fever-associated charged-to-hydrophobic mutation in a human ligand-gated ion channel, allowing us to identify the significance of collective, long-range, electrostatic interactions for maintaining the protein’s function at higher temperatures. The temperature-dependent structural effect of reducing these electrostatic interactions via substitution of K to M at $\gamma 2$: M2 24' can be well-predicted simply by considering Coulombic repulsions between charged residues at M2 24' in all subunits, as well as a simple variational theory which introduces temperature effects. The phenomenon of unstable activation in $\gamma 2$ K289M GABA_{AR}, previously observed *in vivo* and *in vitro*, has now been observed *in silico* and *in principio*.

A basic residue at 24' in the M2-M3 loop is highly conserved across GABA_{AR} subunits, but not across all pLGICs. It is not necessary, however, that charged residues be positioned at 24' for cross-pore repulsions to stabilize open conformations, but simply that they be in the same position in each subunit. Crucial collective interactions might therefore be well indicated by the presence of a charged residue that appears at the same position in all pore-sharing species (i.e. all GABA_{AR} subunits or all GlyR subunits), but which is non-conserved across pLGICs in general.

To maintain the necessary range for cross-pore interactions, it is critical that the charged residues be unscreened. Presence of a nearby oppositely charged residue in one subunit will reduce the charge-charge interaction ($1/r$) to a charge-dipole interaction ($1/r^2$), with presence of an additional charged residue on the other side yielding a dipole-dipole interaction ($1/r^3$). Screening may be affected by changes in pH as well as participation in salt-bridges, suggesting a mechanism that may be crucial for gating in numerous other pLGICs.

Based on these results, we suggest that binding of GABA may activate the channel by reducing screening of residues in the M2 24' ring. In particular, the results of Harrison and co-workers (30) implicate a critical role for interactions between α D57/D14 and α K279 (M2 24'). While it has often been hypothesized that these residues gate by *forming* a salt-bridge, we speculate here that these residues may gate by *breaking* their salt-bridge, removing screening of charged residues in the +5 ring, increasing cross-pore repulsions, and opening the pore.

SUPPLEMENTARY MATERIAL

An online supplement to this article can be found by visiting BJ Online at <http://www.biophysj.org>.

References

1. M. Jaiteh, A. Taly, and J. Hénin, “Evolution of pentameric ligand-gated ion channels: Pro-loop receptors,” *PloS one*, vol. 11, no. 3, p. e0151934, 2016.
2. M. Bianchi and L. Song, “Two different mechanisms of disinhibition produced by GABAa receptor mutations linked to epilepsy in humans,” *The Journal of ...*, vol. 22, no. 13, pp. 5321–5327, 2002.
3. P. Cossette, L. Liu, K. Brisebois, H. Dong, A. Lortie, M. Vanasse, J.-M. Saint-Hilaire, L. Carmant, A. Verner, W.-Y. Lu, Y. T. Wang, and G. a. Rouleau, “Mutation of GABRA1 in an autosomal dominant form of juvenile myoclonic epilepsy,” *Nature genetics*, vol. 31, pp. 184–9, June 2002.
4. J.-Q. Kang, J. Kang, and R. L. Macdonald, “The GABAa receptor gamma2 subunit R43Q mutation linked to childhood absence epilepsy and febrile seizures causes retention of alpha1beta2gamma2S receptors in the endoplasmic reticulum,” *The Journal of neuroscience : the official journal of the Society for Neuroscience*, vol. 24, pp. 8672–7, Oct. 2004.
5. R. L. Macdonald, M. J. Gallagher, H.-J. Feng, and J. Kang, “GABA(A) receptor epilepsy mutations.,” *Biochemical pharmacology*, vol. 68, pp. 1497–506, Oct. 2004.
6. R. W. Olsen and A. J. Tobin, “Molecular biology of GABAa receptors.,” *FASEB J*, vol. 4, pp. 1469–1480, Mar. 1990.
7. R. L. Macdonald and R. W. Olsen, “GABAa receptor channels.,” *Annu Rev Neurosci*, vol. 17, pp. 569–602, 1994.
8. L. E. Rabow, S. J. Russek, and D. H. Farb, “From ion currents to genomic analysis: recent advances in GABAa receptor research.,” *Synapse*, vol. 21, pp. 189–274, Nov. 1995.
9. S. J. Mihic, Q. Ye, M. J. Wick, V. V. Koltchine, M. D. Krasowski, S. E. Finn, M. P. Mascia, C. F. Valenzuela, K. K. Hanson, E. P. Greenblatt, R. A. Harris, and N. L. Harrison, “Sites of alcohol and volatile anaesthetic action on GABA(A) and glycine receptors.,” *Nature*, vol. 389, pp. 385–389, Sept. 1997.
10. D. Belelli and J. J. Lambert, “Neurosteroids: endogenous regulators of the {GABA(A)} receptor.,” *Nat Rev Neurosci*, vol. 6, pp. 565–575, July 2005.
11. E. A. Mitchell, M. B. Herd, B. G. Gunn, J. J. Lambert, and D. Belelli, “Neurosteroid modulation of GABAa receptors: molecular determinants and significance in health and disease.,” *Neurochem Int*, vol. 52, no. 4-5, pp. 588–595, 2008.
12. J. J. Lambert, M. A. Cooper, R. D. J. Simmons, C. J. Weir, and D. Belelli, “Neurosteroids: endogenous allosteric modulators of GABA(A) receptors.,” *Psychoneuroendocrinology*, vol. 34 Suppl 1, pp. S48—S58, Dec. 2009.
13. R. W. Olsen and G.-D. Li, “GABA(A) receptors as molecular targets of general anesthetics: identification of binding sites provides clues to allosteric modulation.,” *Canadian journal of anaesthesia = Journal canadien d'anesthésie*, vol. 58, pp. 206–15, Mar. 2011.
14. E. Sigel, “The benzodiazepine binding site of GABAa receptors,” *Trends in Pharmacological Sciences*, vol. 18, pp. 425–429, Nov. 1997.
15. M. D. Krasowski and N. L. Harrison, “General anaesthetic actions on ligand-gated ion channels.,” *Cell. Mol. Life Sci.*, vol. 55, pp. 1278–1303, Aug. 1999.
16. R. A. Harris, S. J. Mihic, J. E. Dildy-Mayfield, and T. K. Machu, “Actions of anesthetics on ligand-gated ion channels: role of receptor subunit composition.,” *FASEB J*, vol. 9, pp. 1454–1462, Nov. 1995.
17. K. W. Miller, “The nature of sites of general anaesthetic action.,” *Br. J. Anaesth.*, vol. 89, pp. 17–31, July 2002.
18. M. D. Majewska, J.-M. Mienville, and S. Vicini, “Neurosteroid pregnenolone sulfate antagonizes electrophysiological responses to GABA in neurons,” *Neuroscience Letters*, vol. 90, pp. 279–284, Aug. 1988.
19. a. Campos-Caro, S. Sala, J. J. Ballesta, F. Vicente-Agulló, M. Criado, and F. Sala, “A single residue

- in the M2-M3 loop is a major determinant of coupling between binding and gating in neuronal nicotinic receptors.,” *Proceedings of the National Academy of Sciences of the United States of America*, vol. 93, pp. 6118–23, June 1996.
20. J. W. Lynch, S. Rajendra, K. D. Pierce, C. A. Handford, P. H. Barry, and P. R. Schofield, “Identification of intracellular and extracellular domains mediating signal transduction in the inhibitory glycine receptor chloride channel.,” *The EMBO journal*, vol. 16, pp. 110–20, Jan. 1997.
 21. C. Grosman, F. N. Salamone, S. M. Sine, and A. Auerbach, “The extracellular linker of muscle acetylcholine receptor channels is a gating control element.,” *The Journal of general physiology*, vol. 116, pp. 327–40, Sept. 2000.
 22. A. K. Bera, M. Chatav, and M. H. Akabas, “GABA(A) receptor M2-M3 loop secondary structure and changes in accessibility during channel gating.,” *The Journal of biological chemistry*, vol. 277, pp. 43002–10, Nov. 2002.
 23. S. C. R. Lummis, D. L. Beene, L. W. Lee, H. A. Lester, R. W. Broadhurst, and D. A. Dougherty, “Cis-trans isomerization at a proline opens the pore of a neurotransmitter-gated ion channel.,” *Nature*, vol. 438, pp. 248–52, Nov. 2005.
 24. R. J. Law, R. H. Henchman, and J. A. McCammon, “A gating mechanism proposed from a simulation of a human $\alpha 7$ nicotinic acetylcholine receptor.,” *Proc. Natl. Acad. Sci. USA*, vol. 102, pp. 6813–6818, May 2005.
 25. W. Y. Lee and S. M. Sine, “Principal pathway coupling agonist binding to channel gating in nicotinic receptors.,” *Nature*, vol. 438, pp. 243–7, Nov. 2005.
 26. N. Unwin, “Refined structure of the nicotinic acetylcholine receptor at 4~{A} resolution,” *J. Mol. Biol.*, vol. 346, no. 4, pp. 967–989, 2005.
 27. W. Y. Lee, C. R. Free, and S. M. Sine, “Binding to gating transduction in nicotinic receptors: Cys-loop energetically couples to pre-M1 and M2-M3 regions.,” *The Journal of neuroscience : the official journal of the Society for Neuroscience*, vol. 29, pp. 3189–99, Mar. 2009.
 28. R. Sigel, ErwinBuhr, AndreasBaur, “Role of the Conserved Lysine Residue in the Middle of the Predicted Extracellular Loop Between M2 and M3 in the GABA A Receptor.,” *Journal of Neurochemistry*. Oct99, vol. 73, no. 4, 1999.
 29. S. M. O’Shea and N. L. Harrison, “Arg-274 and Leu-277 of the gamma-aminobutyric acid type A receptor alpha 2 subunit define agonist efficacy and potency.,” *The Journal of biological chemistry*, vol. 275, pp. 22764–8, July 2000.
 30. T. L. Kash, A. Jenkins, J. C. Kelley, J. R. Trudell, and N. L. Harrison, “Coupling of agonist binding to channel gating in the GABA(A) receptor.,” *Nature*, vol. 421, pp. 272–5, Jan. 2003.
 31. T. G. Hales, T. Z. Deeb, H. Tang, K. a. Bollan, D. P. King, S. J. Johnson, and C. N. Connolly, “An asymmetric contribution to gamma-aminobutyric type A receptor function of a conserved lysine within TM2-3 of alpha1, beta2, and gamma2 subunits.,” *The Journal of biological chemistry*, vol. 281, pp. 17034–43, June 2006.
 32. R. Macdonald, “Mutations in GABAA receptor subunits associated with genetic epilepsies,” *The Journal of physiology*, 2010.
 33. S. Baulac, G. Huberfeld, I. Gourfinkel-An, G. Mitropoulou, a. Beranger, J. F. Prud’homme, M. Baulac, a. Brice, R. Bruzzone, and E. LeGuern, “First genetic evidence of GABA(A) receptor dysfunction in epilepsy: a mutation in the gamma2-subunit gene.,” *Nature genetics*, vol. 28, pp. 46–8, May 2001.
 34. L. Ramakrishnan and G. P. Hess, “On the mechanism of a mutated and abnormally functioning gamma-aminobutyric acid (A) receptor linked to epilepsy.,” *Biochemistry*, vol. 43, pp. 7534–40, June 2004.
 35. E. Eugène, C. Depienne, S. Baulac, M. Baulac, J. M. Fritschy, E. Le Guern, R. Miles, and J. C.

- Poncer, “GABA(A) receptor gamma 2 subunit mutations linked to human epileptic syndromes differentially affect phasic and tonic inhibition.,” *The Journal of neuroscience : the official journal of the Society for Neuroscience*, vol. 27, pp. 14108–16, Dec. 2007.
36. R. L. Macdonald, J.-Q. Kang, M. J. Gallagher, and H.-J. Feng, “GABA(A) receptor mutations associated with generalized epilepsies.,” *Adv Pharmacol*, vol. 54, pp. 147–169, 2006.
 37. M. O’Mara, B. Cromer, M. Parker, and S.-H. Chung, “Homology model of the GABAA receptor examined using Brownian dynamics.,” *Biophysical journal*, vol. 88, pp. 3286–99, May 2005.
 38. J. Hénin, R. Salari, S. Murlidaran, G. Brannigan, and I. Biology, “A predicted binding site for cholesterol on the GABAA receptor,” *Biophysical journal*, vol. 106, pp. 1938–49, May 2014.
 39. R. E. Hibbs and E. Gouaux, “Principles of activation and permeation in an anion-selective Cys-loop receptor.,” *Nature*, vol. 474, pp. 54–60, June 2011.
 40. W. Humphrey, A. Dalke, and K. Schulten, “VMD: visual molecular dynamics.,” *Journal of molecular graphics*, vol. 14, pp. 33–8, 27–8, Feb. 1996.
 41. A. D. MacKerell, D. Bashford, M. Bellott, R. L. Dunbrack, J. D. Evanseck, M. J. Field, S. Fischer, J. Gao, H. Guo, S. Ha, D. Joseph-McCarthy, L. Kuchnir, K. Kuczera, F. T. Lau, C. Mattos, S. Michnick, T. Ngo, D. T. Nguyen, B. Prodhom, W. E. Reiher, B. Roux, M. Schlenkrich, J. C. Smith, R. Stote, J. Straub, M. Watanabe, J. Wiórkiewicz-Kuczera, D. Yin, and M. Karplus, “All-atom empirical potential for molecular modeling and dynamics studies of proteins.,” *The journal of physical chemistry. B*, vol. 102, pp. 3586–616, Apr. 1998.
 42. J. B. Klauda, R. M. Venable, J. A. Freites, J. W. O’Connor, D. J. Tobias, C. Mondragon-Ramirez, I. Vorobyov, A. D. MacKerell, and R. W. Pastor, “Update of the CHARMM all-atom additive force field for lipids: validation on six lipid types.,” *The journal of physical chemistry. B*, vol. 114, pp. 7830–43, June 2010.
 43. M. C. Pitman, F. Suits, A. D. Mackerell, and S. E. Feller, “Molecular-level organization of saturated and polyunsaturated fatty acids in a phosphatidylcholine bilayer containing cholesterol.,” *Biochemistry*, vol. 43, pp. 15318–28, Dec. 2004.
 44. J. C. Phillips, R. Braun, W. Wang, J. Gumbart, E. Tajkhorshid, E. Villa, C. Chipot, R. D. Skeel, L. Kalé, and K. Schulten, “Scalable molecular dynamics with NAMD.,” *Journal of computational chemistry*, vol. 26, pp. 1781–802, Dec. 2005.
 45. O. S. Smart, J. G. Neduvvelil, X. Wang, B. A. Wallace, and M. S. Sansom, “HOLE: a program for the analysis of the pore dimensions of ion channel structural models.,” *J Mol Graph*, vol. 14, pp. 354–360,376, Dec. 1996.
 46. K. M. Callenberg, O. P. Choudhary, G. L. de Forest, D. W. Gohara, N. a. Baker, and M. Grabe, “APBSmem: A graphical interface for electrostatic calculations at the membrane,” *PLoS ONE*, vol. 5, no. 9, 2010.
 47. T. J. Dolinsky, P. Czodrowski, H. Li, J. E. Nielsen, J. H. Jensen, G. Klebe, and N. A. Baker, “PDB2PQR: expanding and upgrading automated preparation of biomolecular structures for molecular simulations.,” *Nucleic acids research*, vol. 35, pp. W522–5, July 2007.
 48. B. Isralewitz, J. Baudry, J. Gullingsrud, D. Kosztin, and K. Schulten, “Steered molecular dynamics investigations of protein function,” *Journal of Molecular Graphics and Modelling*, vol. 19, no. 00, pp. 13–25, 2001.
 49. S. Park and K. Schulten, “Calculating potentials of mean force from steered molecular dynamics simulations,” *Journal of Chemical Physics*, vol. 120, no. 2004, pp. 5946–5961, 2004.
 50. C. Jarzynski, “Nonequilibrium Equality for Free Energy Differences,” *Physical Review Letters*, vol. 78, pp. 2690–2693, Apr. 1997.
 51. C. Jarzynski, “Equilibrium free-energy differences from nonequilibrium measurements: A master-equation approach,” *Physical Review E*, vol. 56, pp. 5018–5035, Nov. 1997.
 52. J. Hénin and C. Chipot, “Overcoming free energy barriers using unconstrained molecular dynamics

- simulations.,” *The Journal of chemical physics*, vol. 121, pp. 2904–14, Aug. 2004.
- 53. E. Darve, D. Rodríguez-Gómez, and A. Pohorille, “Adaptive biasing force method for scalar and vector free energy calculations.,” *The Journal of chemical physics*, vol. 128, p. 144120, Apr. 2008.
 - 54. A. Pohorille, C. Jarzynski, and C. Chipot, “Good practices in free-energy calculations.,” *J Phys Chem B*, vol. 114, pp. 10235–10253, Aug. 2010.
 - 55. J. Comer, J. C. Gumbart, J. Hénin, T. Lelièvre, A. Pohorille, and C. Chipot, “The Adaptive Biasing Force Method: Everything You Always Wanted to Know, but Were Afraid to Ask.,” *The journal of physical chemistry. B*, Sept. 2014.
 - 56. G. Fiorin, M. L. Klein, and J. Hénin, “Using collective variables to drive molecular dynamics simulations,” *Molecular Physics*, vol. 111, pp. 3345–3362, Dec. 2013.
 - 57. F. Zhu and G. Hummer, “Pore opening and closing of a pentameric ligand-gated ion channel.,” *Proceedings of the National Academy of Sciences of the United States of America*, vol. 107, pp. 19814–9, Nov. 2010.
 - 58. F. Zhu and G. Hummer, “Drying transition in the hydrophobic gate of the GLIC channel blocks ion conduction.,” *Biophysical journal*, vol. 103, pp. 219–27, July 2012.
 - 59. H. Dong, G. Fiorin, V. Carnevale, W. Treptow, and M. L. Klein, “Pore waters regulate ion permeation in a calcium release-activated calcium channel.,” *Proceedings of the National Academy of Sciences of the United States of America*, vol. 110, pp. 17332–7, Oct. 2013.